Asymmetric Epoxidation

DOI: 10.1002/anie.200802223

Functional Analysis of an Aspartate-Based Epoxidation Catalyst with Amide-to-Alkene Peptidomimetic Catalyst Analogues**

*Charles E. Jakobsche, Gorka Peris, and Scott J. Miller**

The biosynthesis of natural products that contain epoxides represents a powerful stimulus for the study of epoxidase enzymes.[1] Likewise, these processes have inspired a generation of science focused on small-molecule catalysts that mediate selective epoxidations through a variety of mechanisms.[2] With respect to the naturally occurring epoxidases, the mechanistic basis of O-atom transfer is often associated with the chemistry of either flavinoid cofactors, P450 enzymes containing a heme group, or chloroperoxidases that lead to stepwise ring formation.[3] In thinking about the known biosynthetic apparatus for epoxide formation, we became curious about an alternative mode for O-atom transfer—one based on functional groups available in proteins, but perhaps not well-documented in the biosynthesis of epoxides. In particular, we speculated and recently showed that aspartic acid containing peptides (e.g., **1**; Scheme 1a) might shuttle between the side-chain carboxylic acid and the corresponding peracid (e.g., **2**) creating a catalytic cycle competent for asymmetric epoxidation with turnover of the aspartate-derived catalyst. Such an approach is orthogonal to the Julia–Colonna epoxidation, a complementary peptide-based epoxidation based on a nucleophilic mechanism.[4] Indeed, as shown in Scheme 1b, this new electrophilic epoxidation catalytic cycle mediates the asymmetric epoxidation of substrates like **3** to give products like **4** with up to 92% *ee*.[5]

Mechanistic questions abound in this catalytic system. To date, we have identified a number of relevant aspects. For example, we observed off-catalytic cycle intermediates, including catalytically inactive diacyl peroxides (**6**).[6] We also showed that these off-cycle intermediates could be reinserted into the productive pathway through the action of nucleophiles such as DMAP or DMAP-*N*-oxide (**7**). On the other hand, the basis of stereochemical information transfer was not immediately clear. Indeed, the high precision delineation of the stereochemical mode of action of chiral catalysts is a critical aspect in the discipline of asymmetric catalysis, whether the catalysts are enzymes or small molecules. With this back-drop, we began a detailed study of the mode of action for catalyst **5**.

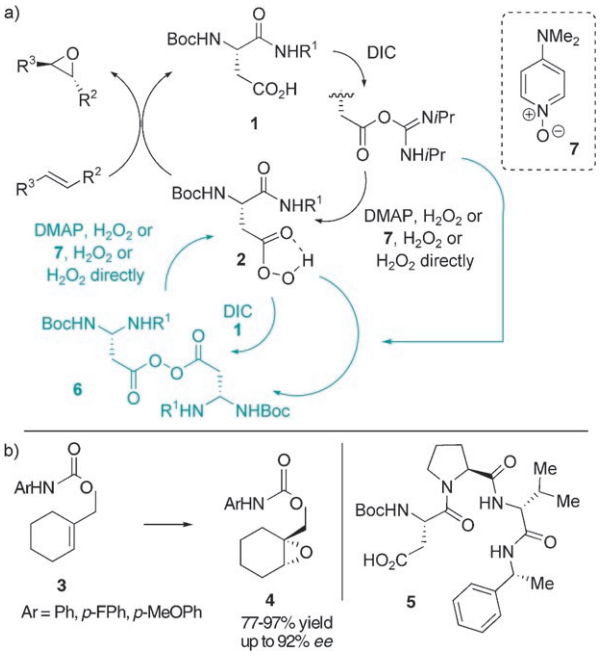

Scheme 1. a) Previously reported catalytic cycle for epoxidation. b) Asymmetric catalytic epoxidation with peptide **5**. Conditions: **5** (10 mol%), DIC (2.0 equiv), DMAP (10 mol%), H_2O_2 (30% aq, 2.5 equiv) or urea–H_2O_2 (2.5 equiv), CH_2Cl_2 or toluene (1.0 M), −10 or 4 °C, 1–3 d. DIC = diisopropylcarbodiimide, DMAP = 4-dimethylaminopyridine.

The conversion of **3** to **4** was originally undertaken with the hypothesis that substrate–catalyst hydrogen bonding might contribute to transition state organization.[7] Indeed, a substrate lacking obvious H-bonding capability (phenylcyclohexene) was found to undergo epoxidation with catalyst **5** with low enantioselectivity (ca. 10% *ee*). Thus, we envisioned several potential loci for contacts between **3** and **5** (Scheme 2a). Shown in blue is the site that represents possible Henbest-type interactions (e.g., ensembles **A** and **B**).[8] Shown in red are other H-bonding sites that might contribute to the preferential formation of **4**. Of these, hand-held models suggested that **C** is consistent with the formation of the major enantiomer. Nevertheless, we sought to interrogate each potential binding site to identify the site(s) of interaction.

To evaluate the importance of the NHBoc functionality, we synthesized catalyst analogue **8**, in which the NHBoc group is replaced with a methyl group.[9] As shown by X-ray crystallography (Scheme 3), analogue **8** adopts the expected Type-II β-turn in the solid state.[10,11] Notably, when catalyst **8** is evaluated in the asymmetric epoxidation of **3** under a

[*] C. E. Jakobsche, G. Peris, Prof. S. J. Miller
Department of Chemistry, Yale University
225 Prospect Street, New Haven, CT 06520-4900 (USA)
Fax: (+1) 203-496-4900
E-mail: scott.miller@yale.edu

[**] We thank the NIH (National Institute of General Medical Sciences) and Merck Research Laboratories, each for partial support.

Supporting information for this article is available on the WWW under http://dx.doi.org/10.1002/anie.200802223.

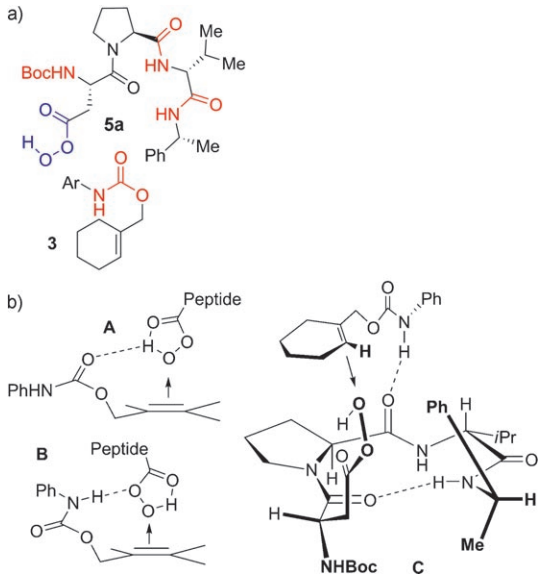

Scheme 2. a) Possible catalyst–substrate H-bonding loci shown in color. b) Representative transition-state ensembles.

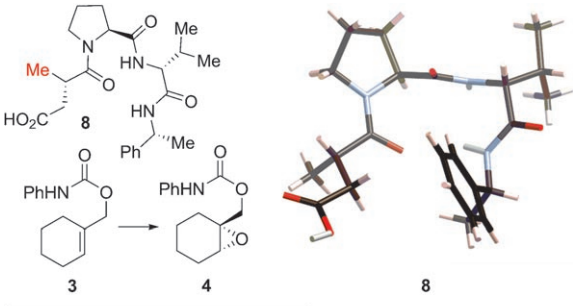

Catalyst	*ee* (e.r.)	Conversion
5[a]	92 (24:1)	76%
5[b]	81 (9.5:1)	63%
8[b]	88 (15.4:1)	26%

Scheme 3. Catalytic performance and X-ray analysis of peptide **8**. Conditions: a) 4 °C, toluene, urea/H_2O_2 complex, DIC, DMAP, 1.0 M, 33 h; b) 23 °C, toluene, 30% H_2O_2, DCC, DMAP, 0.4 M, 12 h. DCC = dicyclohexylcarbodiimide.

common set of conditions (23 °C, toluene, 12 h),[12] product **4** is produced with 88% *ee*, which is analogous to that observed with original catalyst **5**. The fact that peptides **5** and **8** are both selective catalysts suggests that they likely exhibit similar three-dimensional structures. In this vein, the data suggests that the NHBoc group is not involved in an important H-bonding interaction with substrate.

For the functional evaluation of the Pro-D-Val amide, we turned to the application of alkene isosteric replacements of the amide bond.[13] We have previously used this strategy in the mechanistic dissection of peptide-based asymmetric acylation catalysts.[14] We therefore sought to synthesize and study catalyst **9** (Scheme 4a). Peptide **9** was prepared in five steps from known compound **10**.[15,16]

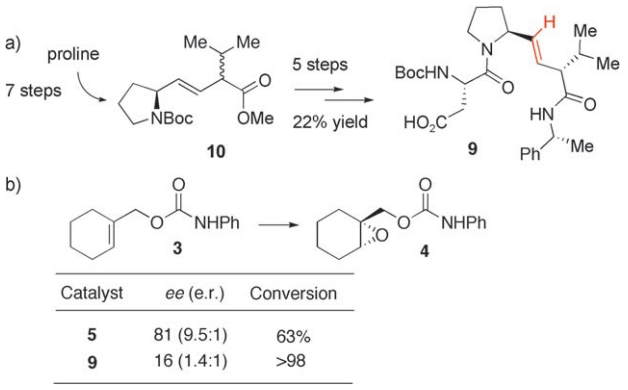

Catalyst	*ee* (e.r.)	Conversion
5	81 (9.5:1)	63%
9	16 (1.4:1)	>98

Scheme 4. a) Synthesis and b) catalytic efficiency of **9**. Conditions: 23 °C, toluene, 30% H_2O_2, DCC, DMAP, 0.4 M, 12 h.

From the functional perspective, catalyst **9** affords a result that suggests that the Pro-D-Val amide could well be involved in a catalyst–substrate H-bond in the transition state. As shown in Scheme 4b, the conversion of **3** to **4** occurs with a much-reduced 16% *ee* under catalysis by peptide **9**. Notably, our observations suggest that self-epoxidation of catalyst **9** is significantly slower than epoxidation of substrate **3** under these conditions.[17]

Perhaps of great significance, however, is the observation that peptidomimetic catalyst **9** exhibits conformational properties that are surprisingly different from catalyst **5**. Whereas catalyst **5** appears as a single conformation in solution by ^{1}H NMR (400 MHz) (Figure 1a), consistent with the β-turn

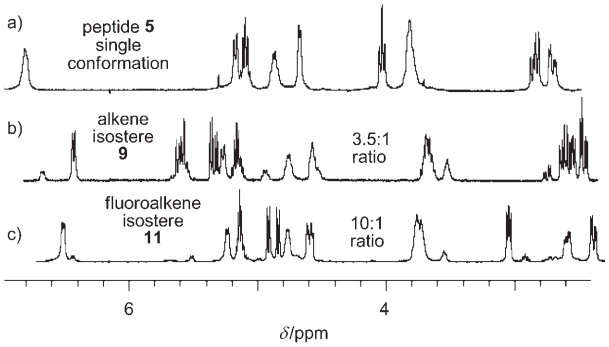

Figure 1. Partial ^{1}H NMR spectra of catalysts **5**, **9**, and **11**.

observed in the X-ray structure of **8**, catalyst **9** appears as a heterogeneous 3.5:1 mixture of two distinct catalyst conformations (Figure 1b). Notably, the signals coalesce when the NMR sample is heated to 100 °C ([D_6]DMSO solvent). Nevertheless, the lack of good homology between the room temperature conformational profiles of catalysts **5** and **9** warranted additional experiments to ascertain the functional role of the Pro-D-Val amide in catalyst **5**.

Whereas dipeptide alkene isosteres have been found to be good steric mimics of amide bonds in peptides and proteins,[18] it is also well-recognized that they provide a poor mimic of other properties intrinsic to amides. In order to recapture amide-like character in an olefinic mimic, dipeptide fluoro-

olefin isosteres have been introduced.[19] In this context, it is also increasingly appreciated that the structural features that cause peptides to adopt secondary structures (including β-turns) are complex. In addition to hydrogen bonding,[20] allylic strain about the Pro-D-Val amide,[21] dipole neutralization of the Pro-D-Val carbonyl,[22] and *n*-to-π* donation[23] from the Xaa-Pro carbonyl lone pair to the Pro-Yaa carbonyl may each contribute to the β-turn's stability.

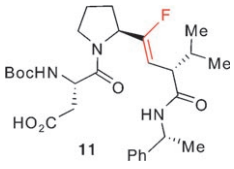

Stimulated by these ideas, we undertook a synthesis of catalyst analogue **11**. Our hypothesis was that the fluoroalkene moiety would be a better mimic of the local properties contributing to faithful β-turn nucleation, and that this catalyst would therefore be a better probe of catalyst **5**.

Scheme 5 shows the synthesis of fluoroalkene isostere **11**.[24] The catalyst was prepared in twenty-one steps and 2% overall yield from phenylalanine (sixteen steps from compound **12**).[9,25] The configuration of enoate **16** was set by a two-step olefination procedure. The stereogenic center in sulfinamide **20** was introduced using an auxiliary-controlled reductive amination.[26] Oxidation of alcohol **22** and coupling to amine **23** gave catalyst **11**.[27]

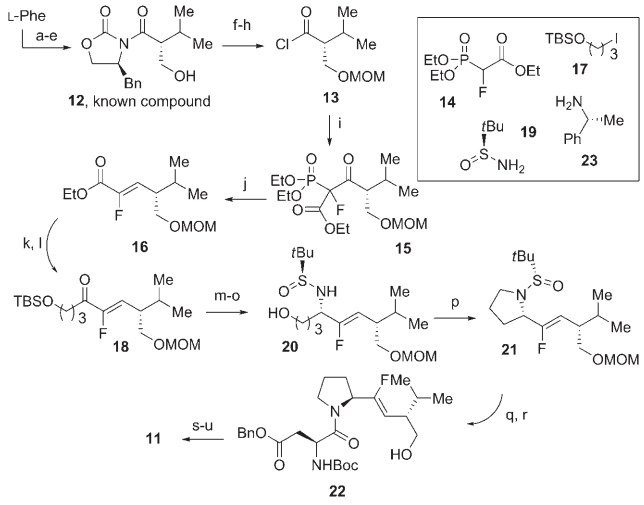

Scheme 5. Synthesis of fluoroalkene isostere **11**: a–e) See Supporting Information; f) DiPEA, MOMCl, CH_2Cl_2, 0 °C, 2.5 h; g) LiOH, H_2O_2, THF, H_2O, 0° to 23 °C, 3 h; h) oxalyl chloride, DMF, diethyl ether, 23 °C, 15 min, 80% yield (3 steps); i) **14**, NaH, THF, 23 °C, 1 h, then **13**, −40 °C, 1 h, (5:1 d.r., use mixture); j) $NaBH_4$, EtOH, −40 °C, 2.5 h, 69% (2 steps, >20:1 d.r.); k) MeNHOMeHCl, *i*PrMgCl, THF, 0 °C, 1.5 h, 79%; l) **17**, diethyl ether, *t*BuLi, −78° to 23 °C, 30 min, then Weinreb amide of **16**, −78 °C, 1 h, 59%; m) **19**, $Ti(OEt)_4$, THF, reflux, 3 h; n) DiBAl-H, −78 °C, 3 h; o) TBAF, THF, 23 °C, 40 min, 95% (3 steps); p) DEAD, PPh_3, THF, 23 °C, 2 h, 80%; q) HCl/dioxane, MeOH, 23 °C, 1.5 h; r) Boc-Asp(OBn)-OH, EDC, HOBt, TEA, CH_2Cl_2, 23 °C, 14 h, 70% (2 steps); s) PDC, DMF, 23 °C, 6 h, 90%; t) **23**, EDC, HOBt, CH_2Cl_2, 23 °C, 14 h, 47%; u) LiOH, dioxane, water, 23 °C, 16 h, 89%. DiPEA = diisopropylethylamine, MOM = methoxymethyl, DiBAl-H = diisobutylaluminum hydride, TBAF = tetrabutylammonium fluoride, DEAD = diethyl azodicarboxylate, EDC = *N*′-(3-dimethylaminopropyl)-*N*-ethylcarbodiimide, PDC = pyridinium dichromate.

Indeed, fluoroalkene **11** proves to be conformationally more robust than alkene-isostere catalyst **9**. Whereas the ^{1}H NMR spectra for catalyst **9** reveal a 3.5:1 conformational mixture (23 °C), fluoroalkene catalyst **11** exhibits an approximately 10:1 mixture of conformations at the same temperature (Figure 1c). Once again, coalescence of the spectrum is observed when the sample is examined by ^{1}H NMR at 100 °C ($[D_6]$DMSO).

Further ^{1}H NMR data (^{1}H-^{1}H NOESY) support the conformational analogies between peptide **5** and the major conformers of both **9** and **11** (Scheme 6). These data suggest that the original peptide and the major conformations of the isosteres adopt β-turn structures similar to that exhibited in the crystal structure of peptide **8** (see Scheme 3).

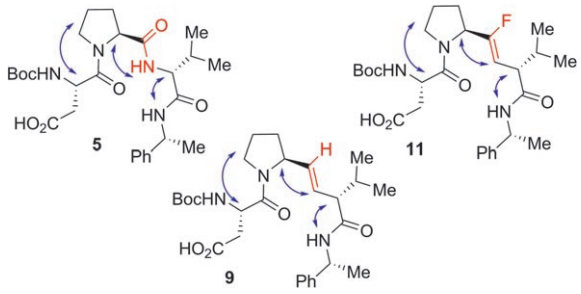

Scheme 6. Select NOE contacts from the major conformational isomers of peptide **5** and its isosteres **9** and **11**.

The actual asymmetric epoxidation reactions catalyzed by **11** offer intriguing results, delivering the product with 52% *ee*—intermediate between the selectivity afforded by catalysts **5** (81% *ee*) and **9** (16% *ee*) under a common set of conditions (Scheme 7).

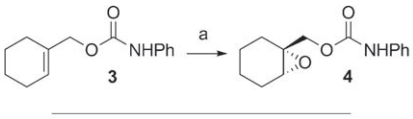

Catalyst	*ee* (e.r.)	Conversion
5	81 (9.5:1)	63%
9	16 (1.4:1)	>98
11	52 (3.2:1)	>98

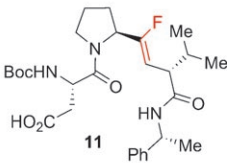

Scheme 7. Catalytic epoxidation data with catalysts **5**, **9**, and **11**. Conditions: a) 23 °C, toluene, 30% H_2O_2, DCC, DMAP, 0.4 M, 12 h.

The intermediate selectivity observed with fluoroalkene isosteric catalyst **11** allows for a number of interpretations. One is that indeed, transition state **C** (Scheme 2b, above) may be the dominant pathway leading to the preferential formation of the major enantiomer in the conversion of **3** to **4**. The near eradication of enantioselectivity with catalyst **9** (16% *ee*) may signal the loss of operation of the dominant pathway, revealing a base level of enantioselectivity through simple shape-selectivity associated with the catalyst. The appearance of partially recovered enantioselectivity with catalyst **11** (52% *ee*; cf. 81% *ee* with **5**), might then be explained by a

weaker, but still significant H-bonding interaction in the transition state involving catalyst **11**. The energetics of C=O···HN hydrogen bonds versus CF···HN have been discussed in the literature, with some debate. Evidence against,[28] and in favor of such interactions has been described.[29] In the present case, the structure–selectivity relationship revealed by catalysts **5**, **9**, and **11** may suggest that a continuum exists with these catalysts (Scheme 8) that is consistent with a moderate, but attractive CF···HN interaction in the dominant transition state.

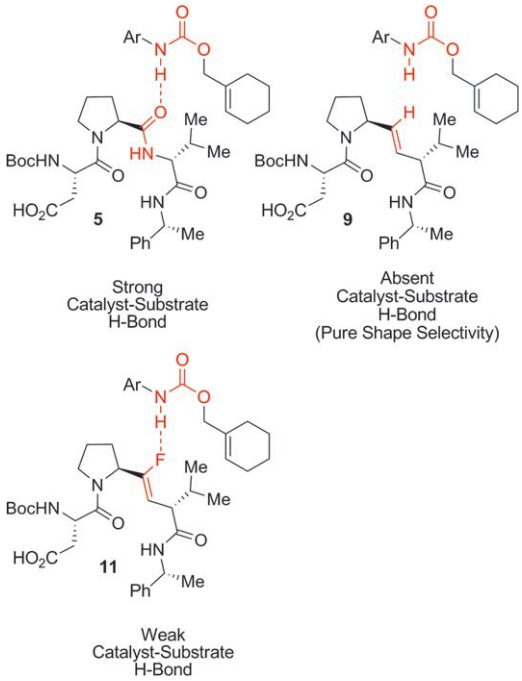

Scheme 8. A potential continuum between catalyst–substrate H-bonding interactions that track with observed enantioselectivity.

Finally, analysis of catalysts with olefinic replacements of the C-terminal amide is not straightforward due to the inevitable eradication of the β-turn structure that such a replacement entails. Nevertheless, catalyst **24**, lacking the C-terminal amide, leads to poor selectivity (16% *ee*; Scheme 9), suggesting an important functional role for this residue. Yet, the lack of conformational analogy between **5**/**9**/**11** and **24** complicates the analysis, in that the role of the C-terminal amide may be purely structural, providing functionality for the signature β-turn H-bonding motif.[17]

Taken together, the experimental results highlight structure–selectivity relationships for a new class of epoxidation catalysts. Through the application of fluorine-substituted alkene isosteres for the mechanistic interrogation of peptide-based catalysts, we have gained several important insights. First, through a comparative study of amide–alkene–fluoroalkene series of catalysts, we have identified unambiguously a hot-spot of correlation between catalyst structure and performance. Moreover, we have shown that such a series may also highlight important conformational features that regulate catalyst conformation, and ultimately

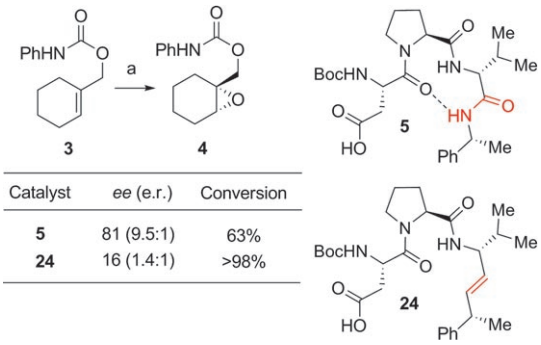

Catalyst	*ee* (e.r.)	Conversion
5	81 (9.5:1)	63%
24	16 (1.4:1)	>98%

Scheme 9. Consequences of C-terminal amide replacements for *ee*. Conditions: a) 23 °C, toluene, 30% H_2O_2, DCC, DMAP, 0.4 M, 12 h.

function. The detailed interrogation of structure–function relationships is a critical step for increasing our understanding of asymmetric catalysis. Mechanistic studies of peptide-based systems may also help to elevate our appreciation of analogies between synthetic catalysts and enzymes, an activity at the heart of biomimetic science.[30]

Received: May 12, 2008
Published online: July 22, 2008

Keywords: asymmetric catalysis · epoxidation · fluorine · olefin isostere · peptides · peptidomimetic

[1] Y. Ding, W. H. Seufert, Q. Beck, D. H. Sherman, *J. Am. Chem. Soc.* **2008**, *130*, 5492–5498.
[2] a) For a recent review of asymmetric epoxidation, see: Q.-H. Xia, H.-Q. Ge, C.-P. Ye, Z.-M. Liu, K.-X. Su, *Chem. Rev.* **2005**, *105*, 1603–1662 See also, b) R. A. Johnson, K. B. Sharpless in *Comprehensive Organic Synthesis*, *Vol. 7* (Ed.: B. M. Trost), Pergamon, New York, **1991**, p. 389; c) E. N. Jacobsen, M. H. Wu in *Comprehensive Asymmetric Catalysis II* (Eds.: E. N. Jacobsen, A. Pfaltz, H. Yamamoto), Springer, Berlin, **1999**, p. 649; d) S. E. Denmark, Z. C. Wu, *Synlett* **1999**, 847–859; e) D. Yang, *Acc. Chem. Res.* **2004**, *37*, 497–505; f) Y. Shi, *Acc. Chem. Res.* **2004**, *37*, 488–496; g) V. K. Aggarwal, C. L. Winn, *Acc. Chem. Res.* **2004**, *37*, 611–620; h) S. Lee, D. W. C. MacMillan, *Tetrahedron* **2006**, *62*, 11413–11424; i) X. Wang, C. M. Reisinger, B. List *J. Am. Chem. Soc.* **2008**, *130*, 6070–6071.
[3] S. Grüschow, D. H. Sherman in *Aziridines and Epoxides in Organic Synthesis* (Ed.: A. K. Yudin), Wiley-VCH, Weinheim, **2006**, p. 349.
[4] a) D. R. Kelly, S. M. Roberts, *Biopolymers* **2006**, *84*, 74–89; b) A. Berkessel, B. Koch, C. Toniolo, M. Rainaldi, Q. B. Broxterman, B. Kaptein, *Biopolymers* **2006**, *84*, 90–96.
[5] a) G. Peris, C. E. Jakobsche, S. J. Miller, *J. Am. Chem. Soc.* **2007**, *129*, 8710–8711; b) A. Berkessel, *Angew. Chem.* **2008**, *120*, 3735–3737; *Angew. Chem. Int. Ed.* **2008**, *47*, 3677–3679.
[6] a) R. P. Jain, J. C. Vederas, *Org. Lett.* **2003**, *5*, 4669–4672; b) J. Rebek, R. McCready, S. Wolf, A. Mossman, *J. Org. Chem.* **1979**, *44*, 1485–1493; c) F. D. Greene, J. Kazan, *J. Org. Chem.* **1963**, *28*, 2168–2171; d) M. D. Spantulescu, R. P. Jain, D. J. Derksen, J. C. Vederas, *Org. Lett.* **2003**, *5*, 2963–2965.
[7] For a review of hydrogen bonding in chiral catalysis, see: A. G. Doyle, E. N. Jacobsen, *Chem. Rev.* **2007**, *107*, 5713–5743.
[8] a) H. B. Henbest, R. A. L. Wilson, *Chem. Ind.* **1956**, *26*, 659; b) P. Kocovsky, I. Stary, *J. Org. Chem.* **1990**, *55*, 3236–3243; c) A. H.

Hoveyda, D. A. Evans, G. C. Fu, *Chem. Rev.* **1993**, *93*, 1307 – 1370.

[9] The details of the synthesis and characterization data can be found in the Supporting Information.

[10] a) G. D. Rose, L. M. Gierasch, J. A. Smith, *Adv. Protein Chem.* **1985**, *37*, 1 – 109; b) T. S. Haque, J. C. Little, S. H. Gellman, *J. Am. Chem. Soc.* **1996**, *118*, 6975 – 6985.

[11] A colorless block crystal ($0.25 \times 0.20 \times 0.20\ mm^3$) was mounted with epoxy cement on the tip of a fine glass fiber. All measurements were made on a Bruker Nonius Kappa CCD diffractometer with graphite monochromated $Mo_{K\alpha}$ radiation. The data were corrected for Lorentz and polarization effects. The data frames were processed and scaled using the DENZO software package. The structure was solved by direct methods and expanded using Fourier techniques. The non-hydrogen atoms were refined anisotropically and hydrogen atoms were treated as idealized contributions. $C_{23}H_{33}N_3O_5{\cdot}CH_2Cl_2 = C_{24}H_{35}Cl_2N_3O_5$ (**8**), $M_r = 516.45\ g\,mol^{-1}$, orthorhombic, space group $P2_12_12_1$ (#19), $a = 9.0028(18)$, $b = 11.376(2)$, $c = 26.325(5)$ Å, $\alpha = 90°$, $\beta = 90°$, $\gamma = 90°$, $V = 2696.1(9)$ Å^3, $Z = 4$, $\rho_{calcd} = 1.272\ g\,cm^{-3}$, $\mu = 2.78\ cm^{-1}$, $Mo_{K\alpha}$ radiation (0.71073 Å), collected at 173(2) K, $2\theta_{max} = 57.90°$, 6950 independent reflections, $R_{int} = 0.0000$, Friedel pairs not merged, $R = 0.0473$, $R_w = 0.0963$, residual electron density = 0.331 and $0.438\ e\,A^{-3}$; CCDC 687520 contains the supplementary crystallographic data for this paper. These data can be obtained free of charge from The Cambridge Crystallographic Data Centre via www.ccdc.cam.ac.uk/data_request/cif.

[12] See Supporting Information for details.

[13] a) J. Gante, *Angew. Chem.* **1994**, *106*, 1780 – 1802; *Angew. Chem. Int. Ed. Engl.* **1994**, *33*, 1699 – 1720; b) R. R. Gardner, G.-B. Liang, S. H. Gellman, *J. Am. Chem. Soc.* **1995**, *117*, 3280 – 3281; c) P. Wipf, T. C. Henninger, S. J. Geib, *J. Org. Chem.* **1998**, *63*, 6088 – 6089.

[14] M. M. Vasbinder, E. R. Jarvo, S. J. Miller, *Angew. Chem.* **2001**, *113*, 2990 – 2993; *Angew. Chem. Int. Ed.* **2001**, *40*, 2906 – 2909.

[15] T. Ibuka, T. Taga, H. Habashita, K. Nakai, H. Tamamura, N. Fujii, *J. Org. Chem.* **1993**, *58*, 1207 – 1214.

[16] Details can be found in the Supporting Information. X-ray data of **9b**: CCDC 687519.

[17] Presumably, intramolecular self-epoxidation requires precise alignment. See: E. J. Corey, H. Niwa, J. R. Falck, *J. Am. Chem. Soc.* **1979**, *101*, 1586 – 1587.

[18] P. Wipf, J. Xiao, S. J. Geib, *Adv. Synth. Catal.* **2005**, *347*, 1605 – 1613.

[19] a) P. A. Bartlett, A. Otake, *J. Org. Chem.* **1995**, *60*, 3107 – 3111; b) S. Couve-Bonnaire, D. Cahard, X. Pannecoucke, *Org. Biomol. Chem.* **2007**, *5*, 1151 – 1157; c) J. J. Urban, B. G. Tillman, W. A. Cronin, *J. Phys. Chem. A* **2006**, *110*, 11120 – 11129.

[20] R. L. Baldwin, *J. Biol. Chem.* **2003**, *278*, 17581 – 17588.

[21] a) R. Deslauriers, J. M. Becker, A. S. Steinfeld, F. Naider, *Biopolymers* **1979**, *18*, 523 – 538; b) D. Q. McDonald, W. C. Still, *J. Org. Chem.* **1996**, *61*, 1385 – 1391.

[22] a) C. Park, W. A. Goddard, *J. Phys. Chem. B* **2000**, *104*, 7784 – 7789; b) E. A. Gallo, S. H. Gellman, *J. Am. Chem. Soc.* **1994**, *116*, 11560 – 11561.

[23] J. A. Hodges, R. T. Raines, *J. Am. Chem. Soc.* **2005**, *127*, 15923 – 15932.

[24] Our synthesis is based on the work of Sano et al. See: S. Sano, Y. Kuroda, K. Saito, Y. Ose, Y. Nagao, *Tetrahedron* **2006**, *62*, 11881 – 11890.

[25] a) R. J. Watson, D. Batty, A. D. Baxter, D. R. Hannah, D. A. Owen, G. J. Montana, *Tetrahedron Lett.* **2002**, *43*, 683 – 685; b) D. L. Boger, J. Hong, *J. Am. Chem. Soc.* **2001**, *123*, 8515 – 8519.

[26] G. Dutheuil, S. Couve-Bonnaire, X. Pannecoucke, *Angew. Chem.* **2007**, *119*, 1312 – 1314; *Angew. Chem. Int. Ed.* **2007**, *46*, 1290 – 1292.

[27] The relative stereochemical relationships were shown by X-ray analysis of the amino alcohol derived from **21** (CCDC 687521). Details of the synthesis can be found in the Supporting Information.

[28] a) J. D. Dunitz, R. Taylor, *Chem. Eur. J.* **1997**, *3*, 89 – 98; b) X. Wang, K. N. Houk, *Chem. Commun.* **1998**, 2631 – 2632.

[29] a) T. J. Barbarich, C. D. Rithner, S. M. Miller, O. P. Anderson, S. H. Strauss, *J. Am. Chem. Soc.* **1999**, *121*, 4280 – 4281; b) H. F. Bettinger, *ChemPhysChem* **2005**, *6*, 1169 – 1174.

[30] J. R. Knowles, *Nature* **1991**, *350*, 121 – 124.

